IMPACT OF WEB PERMEABILITY ON HIGH SPEED WEB TRANSPORT

By

Paul D. Beuther and Neal J. Michal
Kimberly-Clark Corporation
USA

ABSTRACT

Measurements of drag on a moving web in a multi-span festoon show a stronger than expected dependency on the porosity of the web with a highly non-linear relationship. The experiments suggest a wall shear stress 3-4 times larger than non-porous webs or historical Couette flow data for solid walls. Previous DNS studies of boundary layers with passive porous surfaces predict a much smaller increase in wall shear stress for a porous wall of only 40%. Other DNS studies of porous walls with periodic transpiration do show a large increase in drag under certain periodic conditions of modest amplitude. Although those results are more aligned in magnitude with this study, the exact reason for the observed high drag for porous webs in this present study is not understood because there was no external disturbance applied to the web. Previously reported experimental data reported a strong linear correlation between wall shear stress and web permeability. The present paper refines those measurements in more detail and shows a highly non-linear relationship between wall shear stress and permeability, but we offer no physical explanation for this relationship. It can be hypothesized that natural flutter of the web results in a similar mechanism shown in the periodic DNS study, but when the natural flutter was reduced by increasing web tension, there was only a small decrease of the drag.

Because of the prevalence of such flows in many industrial processes using festoons for web accumulation, and the large drag increase that accompanies porous webs, the topic is a very relevant problem. With multiple parallel spans in a festoon, any transpiration in one layer must act in the opposite manner on the adjacent span. This coupling may play a role in the amplification of the drag. Higher drag through a festoon creates processing limitations for light weight porous webs such as non-wovens by restricting maximum speeds or requiring higher than desired web tension to process at high speeds. A festoon is a series of many parallel web paths between idler rolls resulting in a multiple set of planar Couette flows between the moving webs. Length/gap ratios approach 100, with distance between the webs ranging from several millimeters to several hundred millimeters.

NOMENCLATURE

BW	Basis Weight
D	Distance between the moving surfaces
f	Friction Factor
H	Height of festoon carriage
n	number of web strands in festoon = 2 * number of rollers
Re	Reynolds Number, defined using the velocity difference, $\frac{\rho \, \Delta V \, D}{\mu}$
V	velocity of moving surface
ΔV	Magnitude of velocity difference between two web surfaces, = 2V
w	Width of the web
μ	viscosity
ρ	density
τ_w	Turbulent wall shear stress

INTRODUCTION

The majority of forces acting on a moving web are well documented and discernable, but the impact of air drag on transport of permeable webs is shown to not follow expected predictions, as published by Beuther [1]. Air drag values as much as 3X higher than expected were reported. As converting line speeds increase, air drag becomes an increasingly important factor for web tension control, especially where there is a large web surface area such as in long open spans or in festoons. It is important to be able to predict the magnitude of the air drag forces acting on the web in order to maintain good control of web tension, but air drag on permeable webs cannot be easily estimated from previous published experimental studies. While numerous studies exist on turbulent boundary layers relating the wall shear stress, τ_w, to various physical parameters, very few have studied the impact of permeable webs. Most experimental studies of boundary layer flows over permeable surfaces focus on situations with forced flow through the web, either by suction or aspiration. Experiments involving turbulent boundary layer development on permeable webs are rarely published in the literature, and those that have been published do not align with our recent measurements on webs in festoons. DNS studies by Jimenez, et.al. [2] on boundary layers with passive porous surfaces predict an increase in wall shear stress for a porous wall of only 40%. Other DNS studies by Quadrio, et.al. [3] of porous walls with periodic transpiration do show a larger increase in drag under certain periodic conditions of modest amplitude - more aligned in magnitude with these measurements, but under very different conditions. The deviation between expected values and our observations is surprisingly large, and the reason for the difference is not completely understood. Detailed measurements of the boundary layer flow field are needed to better understand the phenomenon.

Most laboratory studies of turbulent Couette flow are conducted on concentric rotating cylinders for ease of operation and size, but this limits the experimentation to studying solid walls with various degrees of roughness. Conversely, all measurements in this study are done on a web moving through a festoon. The flow field in a festoon is a series of planar turbulent Couette flows. Because the aspect ratio of span length H to web spacing D is very large, sometimes exceeding 100, festoons are an excellent platform to measure the effect of web permeability on air drag. The air flow pattern in a festoon is shown schematically in Figure 1, with the distance H shown greatly compressed for easier visualization. Next to it is a schematic of a festoon web path to scale. While the

flow at the end of each span is a deviation from Couette flow due to flow reversal and entrainment, over the majority of the web length the flow is very two-dimensional and fully developed. As will be shown later, any deviations from pure planar flow are easily removed in the data analysis.

Understanding of the dynamics of web behavior in a festoon is not well understood. Kandadai, et.al. [4] published an analysis of wrinkling dynamics in a festoon, but a major area left needing further study was the air/web dynamics within an accumulator. Michal [5] listed air/web interaction within an accumulator as one of the most critical needs for further study.

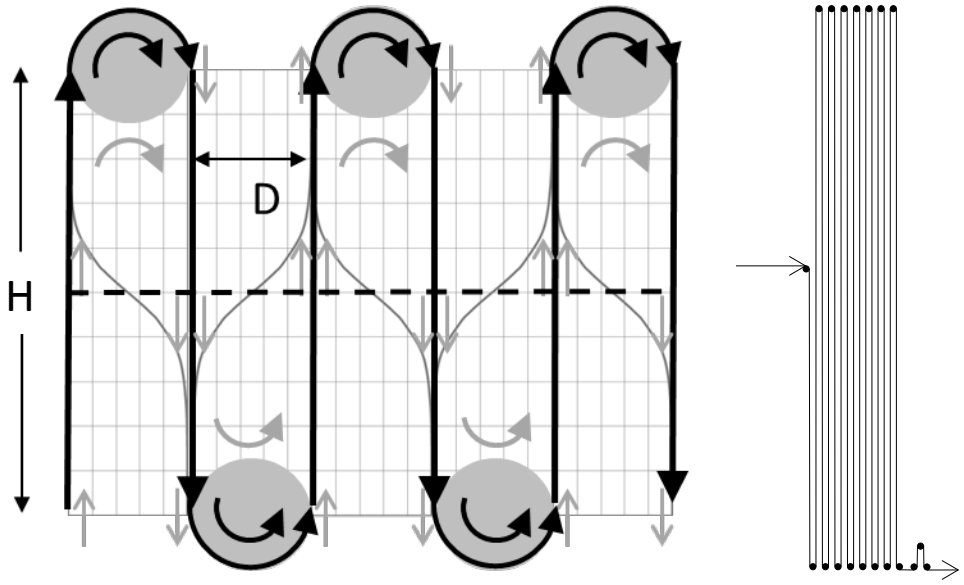

Figure 1 – Schematic of flow patterns in a festoon, and a scaled schematic of the festoon web path

Many experimental studies of turbulent Couette flows have been published. Dorfman [6] published the following result shown in Equation 1 back in 1963 for a smooth wall, relating a friction factor f to the Reynolds number. Figure 2 shows a graphical representation of this relationship.

$$\frac{1}{\sqrt{f}} = 8.13\ \mathrm{Log}\left(Re\sqrt{\frac{f}{2}}\right)+3.49 \qquad \{1\}$$

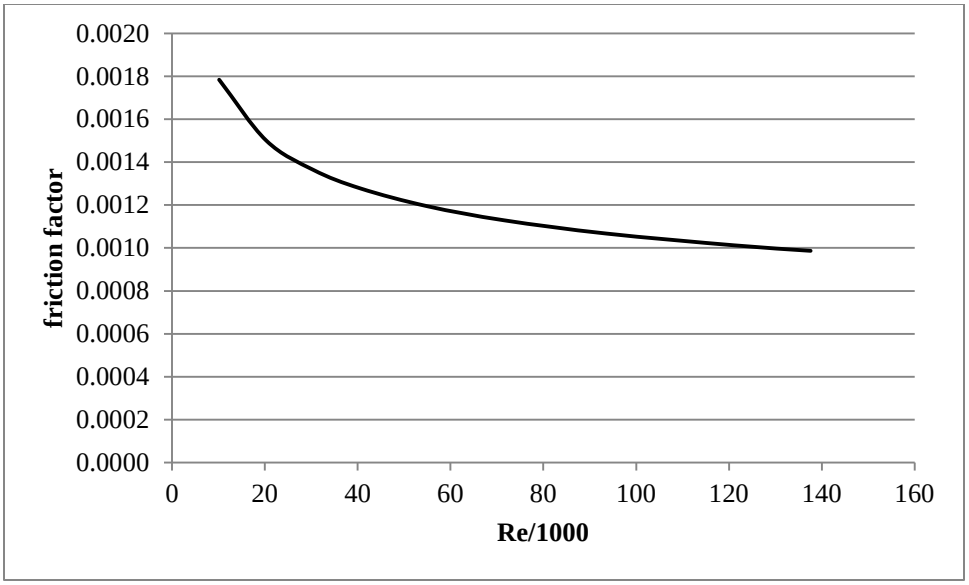

Figure 2 – Friction factor for Turbulent Couette Flow, per Equation 1

The Reynolds number is based on the gap between walls, D, and velocity difference between walls, $\triangle$V. The wall shear stress is related to the friction factor by Equation 2.

$$\tau_w = f\frac{\rho\Delta V^2}{2} \qquad \{2\}$$

It is straight-forward to transfer this to the case of a planar flow where the velocity difference between walls is twice the web speed, since the two webs are moving in opposite directions. This affects the value of the Reynolds number and the wall shear stress when comparing to Dorfman's results. We did not measure actual flows in the festoon, but a CFD simulation was performed for an impermeable web that confirmed the conceptual flow patterns shown in Figure 1, and the calculated wall shear stress matched the result predicted by Dorfman's empirical relationship for a smooth impermeable moving wall.

EXPERIMENTAL PROCEDURE

The focus of our experiments is to measure the tension loss of a web moving through a festoon and relate it to the aerodynamic forces acting on the web, in particular, the wall shear stress. Our primary experimental equipment is a festoon with multiple web strands. The festoon controls the web tension with a pneumatic cylinder that acts on a moving carriage supporting multiple web strands. The carriage has a position sensor that controls the incoming web speed from an upstream unwind by maintaining a set carriage position through a separate control system. Two different festoons were used in the study – one for narrow webs such as would be used on a converting line and the second a wide festoon used in a manufacturing process for non-woven web. The two festoons have 14 or 16 idler rolls respectively, half fixed and half mounted on a vertically moving carriage. The smaller festoon rollers are 28.3 mm (1.115 inches) in diameter and 457 mm (18 inches) long with a spacing of the rollers of 30 mm. The large festoon rollers are 162.5

mm (6.4 inches) in diameter and 3300 mm (130 inches) long with a spacing of the rollers of about 165 mm. When the web is threaded there are either 14 or 16 webs in the festoon, half moving upward and half moving downward. At the maximum extension of the moving carriage, the span length is 2 meters for the small festoon, and 3.5 meters for the large festoon. The average web tension is constant, controlled by the pneumatic cylinder providing a constant upward force on the moving carriage. The tension loss through the festoon is measured by comparing the web tension entering and exiting the festoon with load cells mounted on idlers at the entrance and exit of the festoon.

During steady-state operation, the forces on the web can be characterized as coming from three components – 1) bearing friction of the rollers, 2) air drag on the web at the festoon entrance and exit as well as around the idler rolls, and 3) the air drag on the web due to the planar Couette flow that exists in the center part of the web spans, far from the rollers. While separating the bearing friction from the end effect air drag is not possible with just two load cells, the air drag in the center region can be easily determined. To do so, the web tension at the entrance and exit of the festoon is measured at several different carriage height setpoints. The change in tension loss responds linearly with carriage position, which is directly related to the length of web material in the festoon. By plotting tension loss against the area of web material, we can convert the slope of the line into engineering units of wall shear stress.

The air drag is the integral of the wall shear stress over the area of the moving web. Since the width is constant (ignoring minor web necking), the integral is over the differential length of web. There is also an additional factor of 2 included because there are air drag forces on both sides of the web, so twice the area.

$$Tension\ Loss = \int 2 * Width * \tau_w\, dH + \sum Bearings + \sum Entrance\ \text{Losses} \quad \{3\}$$

The last two terms do not change with carriage height. dH is the change in carriage height, H, multiplied by the number of web strands, *n*, leaving a simple relationship between the wall shear stress and the change in measured tension loss across the festoon as the carriage height is changed. Solving for the wall shear stress yields Equation [4].

$$\tau_w = \frac{1}{2nw}\frac{d}{dH}(Tension\ Loss) \quad \{4\}$$

EXPERIMENTAL RESULTS

Sixteen different materials were evaluated and tension loss data was obtained at several speeds. The materials varied in basis weight from 6 g/m^2 to 22 g/m^2, and had air permeability ranging from 0 to 5.6 m^3/s/m^2 (1094 ft^3/min/ft^2) as measured on a Frasier porosity equipment at 125 Pa pressure drop (1/2 inch H_2O). Each web material was tested on one of our two festoons. In order to compare the results from the two different size festoons used in the study, velocities and spacing between webs are normalized by the Reynolds number.

A representative example of the data from the large festoon is shown in Figure 3. The material is a 14 g/m^2 spunbond measured at two different velocities. The tension loss is graphed in units of force vs. surface area so that the slope of each line equals the wall shear stress in units of Nt/m^2. The x-axis is the festoon height multiplied by the web width and the number of webs, *n*, and times 2 because of the two sides of the web. The y-axis is the tension difference between the exit and entrance of the festoon. The intercept values for each line represent the roller entrance effects and other non-air drag terms that are constant as the festoon height changes. The dashed line in Figure 3 shows the

expected slope for a smooth solid wall for comparison to the 6.35 m/s data. The significant thing about Figure 3 is that the magnitude of the slope of the lines is over four times the expected value, meaning the tension loss on the web due to air drag is over four times higher than would be expected. Air drag on a rough surface instead of a smooth wall cannot come close to accounting for this difference.

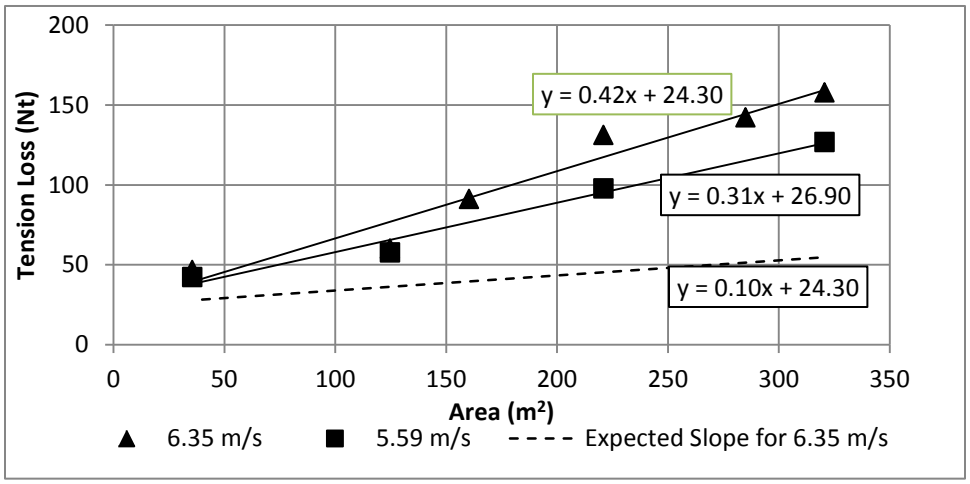

Figure 3 – Festoon Tension Loss

Table 1 provides a summary of the Reynolds numbers studied in these experiments. The smaller festoon was used to evaluate the majority of the web materials. The expected value for the friction factor is the value determined from Equation 1, and the wall shear stress corresponds to the force on the one side of the web.

D (m)	V (m/s)	Re	expected τ_w (Nt/m^2)	expected *f*
0.03	7.62	30,480	0.190	0.00136
0.03	10.16	40,640	0.316	0.00128
0.16	4.32	93,557	0.048	0.00107
0.16	5.59	121,074	0.076	0.00101
0.16	6.35	137,584	0.095	0.00099

Table 1 – Reynolds Number Range of Experiments

Several dozen experiments were run like the one above. The typical festoon height varied from 10% to 90% of the maximum height. Each experiment data provides an estimate of the wall shear stress and friction factor for a given material and Reynolds number. The variability in the measured wall shear stress data is extremely large as shown in Table 3.

Trial	Material	Type	Air Perm ($m^3/s/m^2$)	BW (g/m^2)	Re	measured $\tau_w(N/m^2)$	measured f
1	1	Film/SB	0	30	40,640	0.34	0.00137
2	2	Film	0	16	40,640	0.28	0.00112
3	2	Film	0	16	30,480	0.17	0.00125
4	3	SB/MB	2.4	14	40,640	0.37	0.00150
5	3	SB/MB	2.4	14	30,480	0.18	0.00128
6	4	SMS	2.7	6	40,640	0.38	0.00153
7	4	SMS	2.7	6	30,480	0.16	0.00118
8	5	SB/MB	2.8	12	40,640	0.43	0.00175
9	5	SB/MB	2.8	12	30,480	0.18	0.00127
10	6	SB	3.2	12	40,640	0.55	0.00222
11	7	SB	3.3	14	40,640	0.59	0.00239
12	7	SB	3.3	14	30,480	0.27	0.00192
13	8	SB	3.5	15.3	40,640	0.52	0.00210
14	8	SB	3.5	15.3	30,480	0.19	0.00134
15	9	SB	3.9	14	40,640	0.58	0.00235
16	9	SB	3.9	14	30,480	0.27	0.00192
17	10	SB	4.2	20.3	40,640	0.81	0.00327
18	11	SB	4.4	17.5	40,640	0.81	0.00327
19	12	SB	4.8	14	137,584	0.42	0.00431
20	12	SB	4.8	14	121,074	0.31	0.00409
21	12	SB	4.8	14	93,557	0.11	0.00248
22	13	SB	5.09	15.3	40,640	1.01	0.00407
23	13	SB	5.09	15.3	30,480	0.45	0.00326
24	14	SB	5.13	17.5	40,640	0.92	0.00371
25	15	BCW	5.5	22	40,640	1.30	0.00526
26	15	BCW	5.5	22	30,480	0.61	0.00440
27	16	SB	5.6	8	40,640	1.15	0.00464
28	16	SB	5.6	8	30,480	0.56	0.00401

Table 2 – List of Materials and Experimental Data

It is hypothesized that the air permeability of each web material can explain away much of the variability. Figure 4 partially confirms this hypothesis by combining all the data into one graph, with wall shear stress (air drag) plotted against the air permeability of the material for each Reynolds number. For materials with zero permeability, the wall shear stress agrees well with expected values as shown by the dashed lines for each Re. For materials with non-zero permeability, the wall shear stress exceeds the expected value, often by a factor of more than 4, and in a non-linear relationship with permeability. For the two sets of data at Re=30,480 and Re=40,640 where numerous materials were tested, the wall shear stress increases with air permeability to about the power of 3. This is contrary to results published previously by Beuther [1] that suggested a linear trend. The non-linearity is clearly shown in the current data due to the greater number of

materials included in this data set. There is still a data gap in the region between 0 and 2.5 $m^3/s/m^2$, and the data hints that the trend may not be a smooth polynomial curve as shown, especially for the lower Reynolds number data, but perhaps a more like a threshold limit, where the increase in drag is minimal until a certain threshold in permeability is reached. However, since the mechanism for the increased drag is not yet understood, this is merely conjecture.

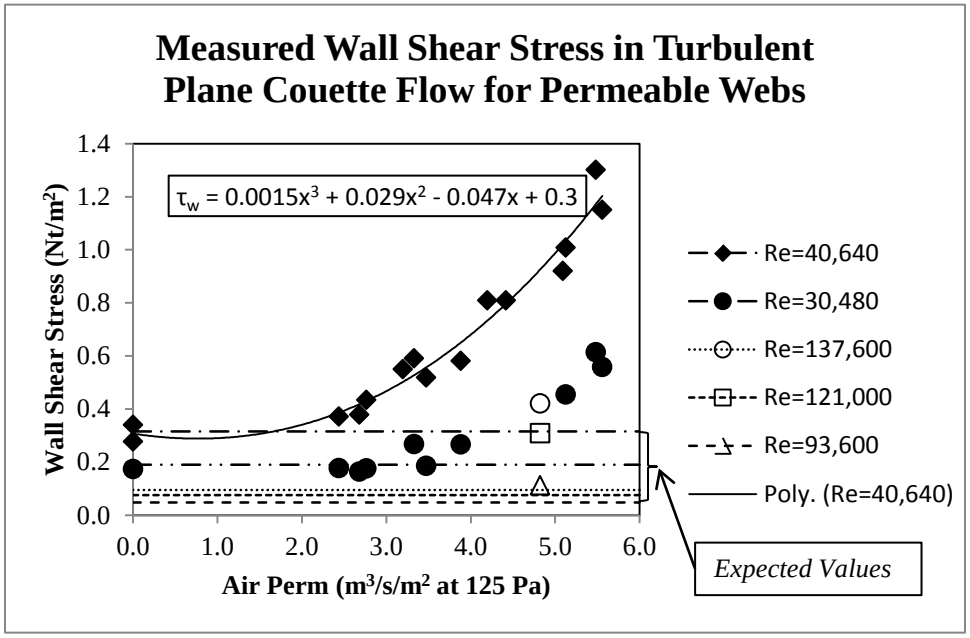

Figure 4 – Wall Shear Stress vs. Air Permeability

Because the wall shear stress is dependent on ΔV^2, the data in Figure 4 does not collapse well. A much better collapse of the data is shown in Figure 5 with the data plotted as the friction factor vs. air permeability. The drag increase for several of the materials is greater than four times that of a smooth wall. Higher air permeability drives this increase. A slight trend with Reynolds number also exists, although the lowest velocity data from the large festoon (Re = 93,600) does not match the Reynolds number trend and is lower than expected. Our hypothesis is that there are other scaling factors that we have not considered that are related to the velocity or permeability, and not just the Reynolds number based on the web speed and web spacing.

Web flutter is another parameter that may be relevant, but other trials not shown here showed little difference in air drag when web tension was increased. If web flutter were important, a change in tension should have reduced flutter and changed the air drag. It did not, so the lack of response points away from this hypothesis. Air lubrication at the rollers is also not a factor because it is the same at each festoon height, as the H/D ratio is large enough to ensure a fully developed Couette flow.

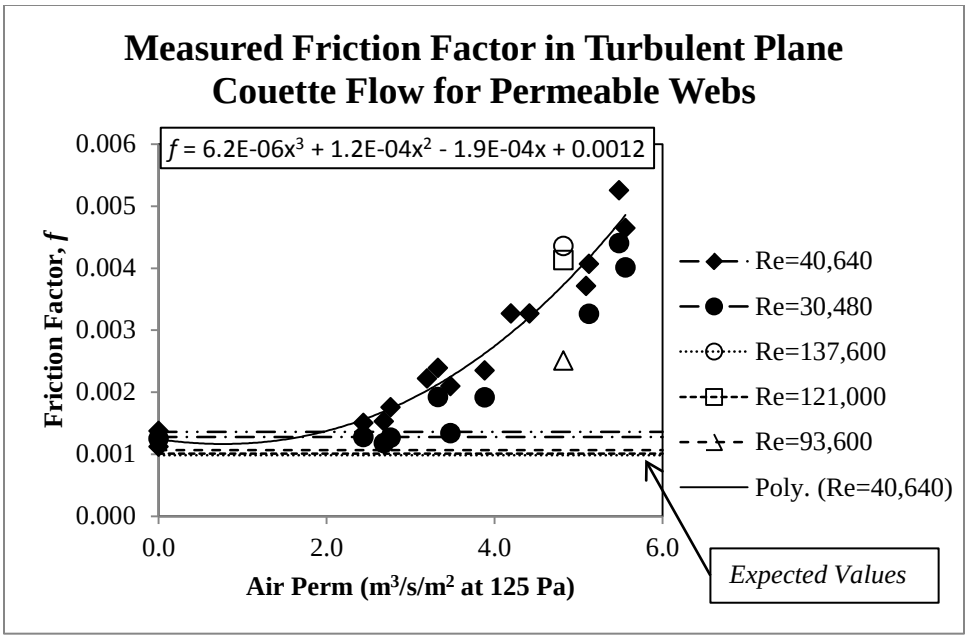

Figure 5 – Impact of Web Permeability on Drag

CONCLUSIONS

Results presented here show that air permeability of a web is an important parameter for web handling dynamics in festoons. Previous understanding of the impact of web air permeability was limited to traction on rollers due to air film lubrication, but that impact is applicable to low or zero permeable webs. The results shown here deal with the opposite end of the permeability spectrum where the air film development on rollers is not an issue. Increases in air drag on highly permeable webs can have disastrous effects on web handling due to high tension losses, especially at higher speeds. It is admittedly puzzling that the increase in drag with permeability is so highly non-linear, and that the magnitude is so large. It is hoped that others will continue to study the aerodynamics of these flow fields to determine the dynamics of the turbulent boundary layer that cause this increase. We hypothesize that the web permeability allows for a strong transport of turbulent energy from one flow stream to another on the opposite side of the web, but the dynamics of this are complex and not understood at this time. The proper scaling is unlikely to be the Reynolds number based on the gross dimensions like the spacing, but instead include micro-scale dimensions of the boundary layer.

REFERENCES

1. Beuther, P. D., "Measurements of Wall Shear Stress in a Planar Turbulent Couette Flow with Porous Walls," presented at the annual meeting of the APS/DFD, published in the Bulletin of the American Physical Society, Vol, 58, No.18, November 2013.
2. Jimenez, J., Ulhmann, M., Pinelli, A., and Kawahara, G., "Turbulent Shear Flow over Active and Passive Porous Surfaces," J. Fluid Mech., Vol 442, 2001, pp. 89-117.

3. Quadrio, M., Floryan, J. M., and Luchini, P., “Effect of Streamwise-Periodic Wall Transpiration on Turbulent Friction Drag,” J. Fluid Mech. Vol. 576, 2007, pp. 425-444.
4. Kandadai, B. K., Michal, N. J., and Patil, A., “Analysis of Web Wrinkling in Accumulators,” Proceedings of the Eleventh International Conference on Web Handling, June 12-15, 2011, pp. 339-364.
5. Michal, Neal J., “Web Tension in an Accumulator and Industry Needs for the Future,” Proceedings of the Tenth International Conference on Web Handling, June 7-10, 2009, pp. 219-233.
6. Dorfman, L. A., Hydrodynamic Resistance and the Heat Loss of Rotating Solids, Edinburgh, Oliver and Boyd, 1963.